Mitman, Jeffrey

From: Mitman, Jeffrey NRR
Sent: Tuesday, June 01, 2010 3:08 PM
To: Philip, Jacob; Nicholson, Thomas
Subject: NSAC/60
Attachments: NSAC-60.pdf

The pertinent sections of NSAC/60 are in the attached. The document vitals are:

NSAC/60
Oconee PRA
A Probabilistic Risk Assessment of Oconee Unit 2
The Nuclear Safety Analysis Center of EPRI and Duke Power Company
1984

105

9.4 ANALYSIS OF EXTERNAL FLOOD EVENTS

This section presents results of analyses performed to evaluate the contribution of external floods to the core-melt frequency estimated for Oconee Unit 3. It also explains in detail the methods used in these analyses.

Two potential sources of external flooding of the Oconee plant were identified. The first is a general flooding of the rivers and reservoirs in the area due to rainfall in excess of the probable maximum precipitation (PMP). Since the Oconee site is inland, the effects of hurricanes were not considered. The second source is a random failure of the upstream Jocassee Dam. (Random failure includes all causes other than a rain-induced overtopping and an earthquake-induced failure, which were analyzed explicitly).

9.4.1 PRECIPITATION

The PMP postulated for the Oconee site would be 26.6 inches within 48 hours. The effects of this PMP on reservoirs and spillways were evaluated in a study performed by the Duke Power Company (1966). The results of this study demonstrated that the Keowee and Jocassee reservoirs are designed to contain and control the floods that could result from a PMP. Thus in order to flood the plant site, rainfall exceeding the PMP must occur. The frequency of exceeding the PMP was obtained from the analysis presented in this section and was used as a bounding estimate of the frequency of core melt caused by rain-induced external flooding.

9.4.1.1 Precipitation Data

The U.S. Weather Bureau (1961, 1964) has compiled a series of rainfall intensity-duration-frequency curves derived from meteorological data collected throughout the continental United States over a period of 50 years. The isopluvial maps published in these technical papers were interpolated for the Oconee site to obtain the amount of precipitation (inches) given the rainfall duration (hours) and its annual frequency of occurrence. The interpolated data for the Oconee site (see Table 9-18) are the basis for all the results derived in this section.

9.4.1.2 Method

The method used in deriving the probability distribution of the frequency for a PMP is an extension of the technique of Bayesian extrapolation first developed by S. Kaplan (personal communication, 1981). This method extrapolates the known trend to values outside those experienced to date. It is particularly suitable for probabilistic analyses because it establishes the degree of confidence in the extrapolation--providing that the trend continues. The validity of the assumption of a continuing trend is discussed in Section 9.4.1.5.

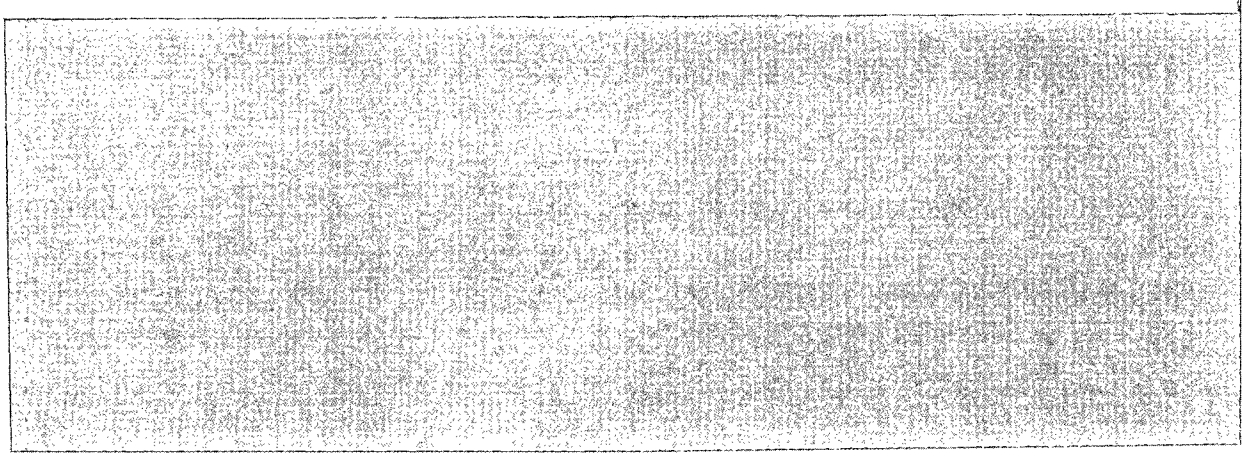

Table 9-18. Input Data for the Oconee External Flood Analysis[a]

Data point, m	Rainfall duration, τ_m (hours)	Precipitation depth, h_m (inches)	Observed storm frequency, f_m^o (yr-1)	Number of observed storms in 50 years $\nu_m^o = 50\ f_m^o$
1	12	3.5	1.0	48
2	12	4.2	0.5	24
3	12	4.8	0.2	10
4	12	5.8	0.1	5
5	12	6.7	0.04	2
6	12	7.5	0.02	1
7	12	8.1	0.01	1
8	24	4.2	1.0	48
9	24	4.7	0.5	24
10	24	6.5	0.2	10
11	24	6.8	0.1	5
12	24	8.5	0.04	2
13	24	9.2	0.02	1
14	24	10.5	0.01	1
15	48	6.0	0.5	24
16	48	7.0	0.2	10
17	48	8.0	0.1	5
18	48	9.5	0.04	2
19	48	10.0	0.02	1
20	48	11.5	0.01	1
21	96	7.0	0.5	24
22	96	8.5	0.2	10
23	96	10.0	0.1	5
24	96	11.0	0.04	2
25	96	12.0	0.02	1
26	96	14.0	0.01	1
27	168	8.5	0.5	24
28	168	10.0	0.2	10
29	168	13.0	0.04	2
30	168	14.0	0.02	1
31	168	16.0	0.01	1

[a]Obtained by interpolation of U.S. Weather Bureau isopluvial maps.

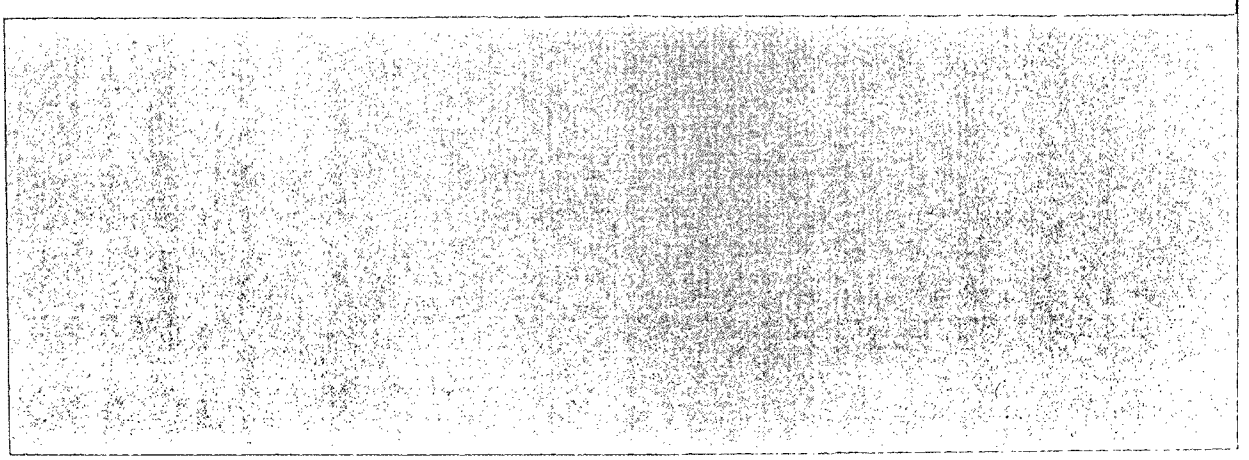

A plot of the data presented in Table 9.18 is shown in Figure 9-56. This plot shows that there is a family of curves predicting the frequency of a rainstorm for the Oconee site in terms of the cumulative precipitation and the duration of the storm. The family of curves suggest that the frequency can be expressed as an exponential function of the form

$$c_{f(\tau,h)} = a \exp\{-[B(\tau)h]\} \qquad (9.4\text{-}1)$$

where

$c_{f(\tau,h)} \equiv$ calculated frequency of storm (yr^{-1})
$h \equiv$ maximum cumulative precipitation (in)
$\tau \equiv$ duration of rainfall (hr)
$a \equiv$ constant cumulative precipitation (in)
$B(\tau) \equiv$ a function of τ

Analysis of the $B(\tau)$ values obtained by fitting each individual curve of Figure 9-56 suggests that $B(\tau)$ can be expressed as

$$B(\tau) = b/\tau^n \qquad (9.4\text{-}2)$$

where n is a constant.

Substituting Equation 9.4-2 into Equation 9.4-1 gives

$$c_{f(\tau,h,a,b,n)} = a \exp\{-[b(h/\tau^n)]\} \qquad (9.4\text{-}3)$$

where for emphasis f is expressed as a function of a, b, and n.

Equation 9.4-3 expresses a mathematical model for the frequency of a complicated meteorological process involving many random variables. This model along with the data in Table 9-18 was used to derive probabilities for the various combinations of values for a, b, and n.

This set of probabilities permits the derivation through Equation 9.4-3 of the probability distribution for the frequency of PMP (τ_{PMP} = 48 hr; h_{PMP} = 26.6 in.).

Table 9-18 consists of 31 data entries. Each entry (m) represents the observed number of storms (ν_m^o) exhibiting particular values of cumulative precipitation (h_m) and duration (τ_m) over the 50-year observation period. The quantity ν_m is defined by

$$\nu_m = 50\ f_m^o \qquad (9.4\text{-}4)$$

where f_m^o is the observed frequency for entry (m).

For each of these entries, a doublet,

$$E_m = \langle \nu_m^o, 50 \rangle$$

can be formed to characterize the experience E_m.

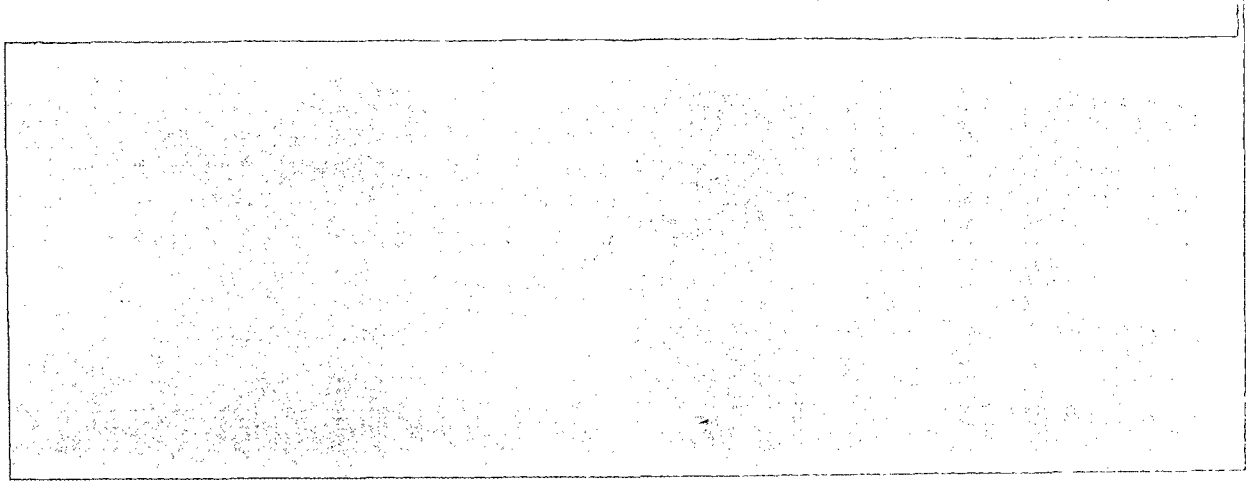

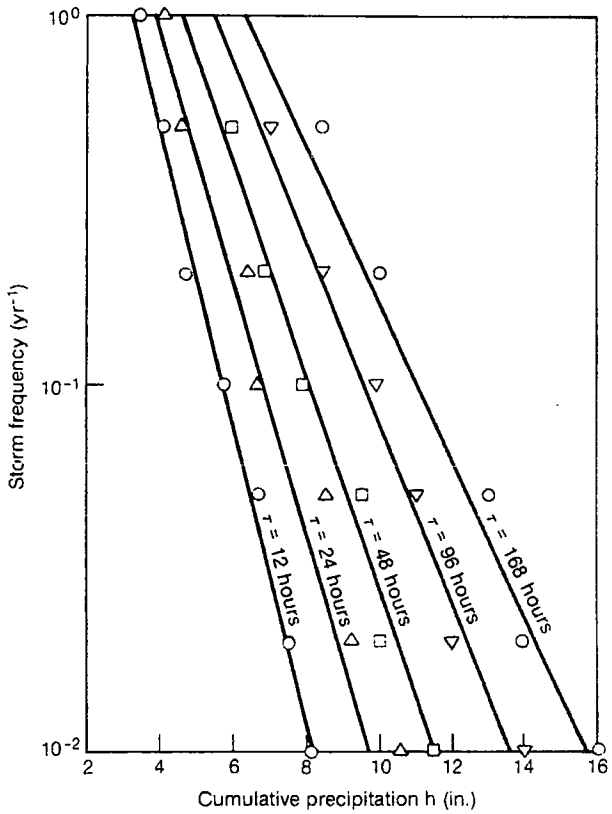

Figure 9-56. Plot of the data in Table 9-18. (Solid lines are a fit of data to Equation 3.)

The collective experience E of all 31 data points can be characterized by

$$E \equiv \{<\nu_m^o, 50>\} \text{ all } m \tag{9.4-5}$$

In light of this evidence E and Equation 9.4-3 (which models the frequency f), a probability was assigned to the various combinations of different values for the three unknown parameters a, b, and n, using Bayes' theorem:

$$p(a,b,n|E) = p(a,b,n) \frac{p(E|a,b,n)}{\sum_{\substack{\text{all} \\ a,b,n}} p(E|a,b,n)} \tag{9.4-6}$$

where

$p(a,b,n) \equiv$ probability of a, b, and n prior to experience E
$p(E|a,b,n) \equiv$ likelihood of a, b, and n after the experience E
$p(a,b,n|E) \equiv$ probability of a, b, and n after the experience E

To obtain information on the probability of a, b, and n, several steps must be taken. The first is to define the calculated number of storms (c_ν) during the 50-year observation period:

$$c_{\nu(\tau,h,a,b,n)} = 50 c_{f(\tau,h)} \tag{9.4-7}$$

where $c_{f(\tau,h)}$ is given by Equation 9.4-3.

The likelihood of observing the doublet

$$E_m \equiv <\nu_m^o, 50>$$

given the values a, b, and n, can now be formulated. A process describing events that occur randomly in time is characterized by the Poisson distribution. This distribution predicts the likelihood of observing the doublet E_m given a, b, and n:

$$p(E_m|a,b,n) = \frac{\left[c_{\nu(\tau_m,h_m,a,b,n)}\right]^{\nu_m^o}}{\nu_m^o!} \exp\left[-c_{\nu(\tau_m,h_m,a,b,n)}\right] \tag{9.4-8}$$

The likelihood of the total experience E is the product of the likelihoods of all the individual E_m terms--that is,

$$\begin{aligned} p(E|a,b,n) &= \prod_{\substack{\text{all} \\ m}} p(E_m|a,b,n) \\ &= \prod_{\substack{\text{all} \\ m}} \frac{\left[c_{\nu(\tau_m,h_m,a,b,n)}\right]^{\nu_m^o}}{\nu_m^o!} \exp\left[-c_{\nu(\tau_m,h_m,a,b,n)}\right] \end{aligned} \tag{9.4-9}$$

With the $p(E|a,b,n)$ defined, the prior probability distribution $p(a,b,n)$ is needed before applying Equation 9.4-6 to calculate $p(a,b,n|E)$. Since there was no knowledge prior to experience E on the probability of the different

possible combinations of values for a, b, and n, a uniform prior was assumed, and Equation 9.4-6 is rewritten as

$$p(a,b,n|E) = \frac{p(E|a,b,n)}{\sum_{\substack{\text{all}\\a,b,n}} p(E|a,b,n)} \qquad (9.4\text{-}10)$$

where $p(E|a,b,n)$ is given by Equation 9.4-9.

9.4.1.3 Numerical Analysis

Equation 9.4-3 expresses the frequency of a storm of duration (τ_m) and cumulative precipitation depth (h_m) for any given combination of a, b, and n. Equation 9.4-10, on the other hand, establishes the probability of a specific combination of values a, b, and n in light of the available data. The objective of the numerical analysis was to obtain from these two equations the probability distribution for storm frequencies for a specific τ and h (i.e., at the PMP conditions).

The numerical procedure requires establishing a grid of a_i, b_j, n_k values for a discrete evaluation of $p(E|a,b,n)$ and subsequently $p(a,b,n|E)$. A judicious choice of grid points is essential in obtaining accurate results without excessive computation. The following grid was used in evaluating the data of Table 9-18:

$$\{[a_i]\} = \{10,15,20,25,30,35,40,45,50,55,60\}$$

$$\{[b_j]\} = \{1.0,1.1,1.2,1.3,1.4,1.5,1.6,1.7,1.8,1.9,2.0.2.1,2.2,2.3,2.4,2.5,2.6\}$$

$$\{[n_k]\} = \{0.10,0.12,0.14,0.16,0.18,0.20,0.22,0.24,0.26,0.28,0.30,0.32,0.34,0.36,0.38,0.40\}$$

For each specific combination of a_i, b_j, n_k values from this grid one can evaluate Equation 9.4-9, the likelihood function, which when expressed in its discrete form is given by

$$p(E|a_i,b_j,n_k) = \prod_{\substack{\text{all}\\m}} \frac{[c_{\nu}(\tau_m,h_m,a_i,b_j,n_k)]^{\nu_m^o}}{\nu_m^o!} \exp[-c_{\nu}(\tau_m,h_m,a_i,b_j,n_m)] \qquad (9.4\text{-}11)$$

The posterior probability for each a_i, b_j, n_k combination can now be obtained from a discrete form of Equation 9.4-8:

$$p(a_i,b_j,n_k|E) = \frac{p(E|a_i,b_j,n_k)}{\sum_{\substack{\text{all}\\i}} \sum_{\substack{\text{all}\\j}} \sum_{\substack{\text{all}\\k}} p(E|a_i,b_j,n_k)} \qquad (9.4\text{-}12)$$

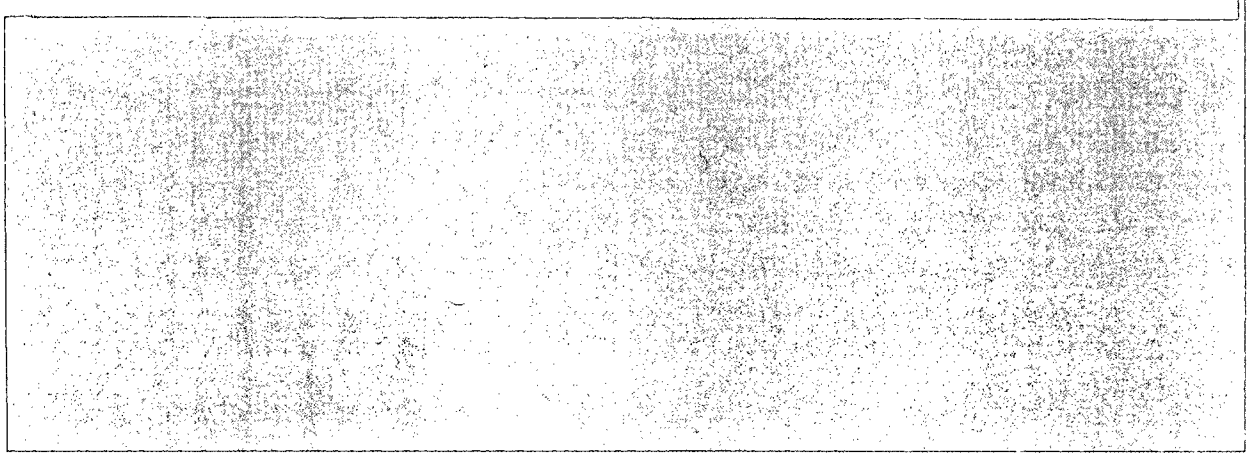

The last step of the analysis is the evaluation of the discrete version of Equation 9.4-3 at each one of the grid points

$$c_{f,ijk} = a_i \exp\left(-\frac{b_j h_{PMP}}{\frac{n_k}{\tau_{PMP}}}\right) \qquad (9.4\text{-}13)$$

where τ_{PMP} is the duration of a PMP rainfall (48 hours) and h_{PMP} is the maximum cumulative precipitation of a PMP rainfall (26.6 inches).

Note that for each $c_{f,ijk}$ there is a corresponding $p(a_i, b_j, n_k|E)$. In probabilistic language this correspondence is called a "doublet."[k] The entire set of

$$\{\langle p(a_i, b_j, n_k|E),\ c_{fijk}\rangle\}$$

doublets forms the probability distribution for the frequency of the PMP storm at the Oconee site. The cumulative of this discrete probability distribution indicates the confidence when postulating a particular storm-frequency value.

9.4.1.4 Results

The numerical analysis described in Section 9.4.1.3 was carried out with the objective of calculating the probability distribution for the PMP frequency. A computer program specifically designed to carry out this analysis was written in the Basic language. The results of these calculations are given in Table 9-19: the PMP storm-frequency intervals, the discrete probability distribution (DPD) for each interval, and finally, the cumulative probability from zero to the end of each frequency interval.

Table 9-19. Probability Distribution for the Frequency of PMP Storms[a]

Storm-frequency range			
From	To	DPD	Cumulative probability
0	3.5-8[b]	0.0253	0.0253
3.5-8	6.0-8	0.0429	0.0682
6.0-8	1.0-7	0.1413	0.2096
1.0-7	1.7-7	0.2283	0.4380
1.7-7	3.0-7	0.2850	0.7230
3.0-7	5.0-7	0.1104	0.8334
5.0-7	8.0-7	0.0941	0.9276
8.0-7	1.3-6	0.0428	0.9704
1.3-6	2.2-6	0.0267	0.9972

[a]Duration τ = 48 hours; precipitation depth h = 26.6 inches.
[b]3.5-8 = 3.5×10^{-8}.

A least-squares fit of the Table 9-19 storm frequency versus cumulative probability yields the frequencies of a PMP associated with the lower, median, and upper bounds of the probability distribution:

Cumulative probability	PMP frequency ($year^{-1}$)
0.05	4.9-8
0.50	2.9-7
0.95	8.9-7

The cumulative probability for a particular frequency interval is to be interpreted as the degree of certainty that the PMP frequency observed over a long period of time will be less than or equal to the upper value of that frequency interval.

9.4.1.5 Discussion and Conclusions

Three questions concerning the validity of this analysis come to mind. First, since the data on which the analysis is based were collected during a relatively short period, 50 years, how can we be sure that the climatic conditions prevailing today will continue indefinitely?

For the purpose of this analysis there is no need to know that the prevailing climatic conditions will continue any longer than the plant life (about 40 years). The PMP frequency results are then based on the expectation that no dramatic change in climatic conditions will occur over the next 40 years. Historical data on climate show this assumption to be reasonable.

Second, we have formulated a mathematical model, Equation 9.4-3, which predicts the frequency of a storm given the duration of rainfall (hours) and the cumulative precipitation (inches). How can we be certain that this exponential model still applies at the precipitation level of a PMP storm?

We have no way of being certain that the exponential model continues to apply at the precipitation level of a PMP storm. The amount of precipitation during a period of time is dependent on a variety of random meteorological variables. The severity of the rainstorm is related to the probability of occurrence of increasingly adverse conditions (exponential model). There are, however, physical limits on these adverse conditions; at those limits the exponential model breaks down. If we continue to use the exponential model beyond those limits, we will overpredict the frequency of the storms. Since there is no information beyond the recorded data as to where the exponential model breaks down, the results of this analysis are an upper-bound, conservative estimate of the frequency of a PMP storm.

Third, there is an implicit assumption that the most severe condition that can affect the area around the Oconee site is the one where the storm lasts 48 hours with a cumulative precipitation of 26.6 inches. Is this truly the limiting storm, or could other storms of shorter or longer duration possibly cause flooding at the Oconee plant?

The duration, cumulative precipitation, and frequency resulting from this analysis have been reviewed by the plant designers and they share the belief of the Duke Power Company (communication from S. B. Hager, August 18, 1981), that the PMP storm is the most frequent storm that could exceed spillway capacities and result in flooding of the plant site.

Since the conservatively calculated mean frequency of flooding of the Oconee plant due to the PMP storm is more than an order of magnitude less than that due to a random failure of the Jocassee Dam, it was concluded that precipitation-induced external flooding is a negligible contributor to core-melt frequency and public risk.

9.4.2 DAM FAILURE

The Oconee site has a yard grade elevation a few feet below the full-pond level of Lake Keowee, which serves as the source of its condenser circulating water. Lake Jocassee has a full-pond elevation about 300 feet above Lake Keowee. If a sudden failure of the Jocassee Dam were to occur, and a rapid enough release of the impounded water from Lake Jocassee into Lake Keowee resulted, the flood wave generated in Lake Keowee would overtop the Keowee Dam and the Oconee intake dike, flooding the plant. This section presents the analysis performed to estimate the frequency of such a flood.

9.4.2.1 Frequency of Dam Failure

The Jocassee Dam is an earth-rockfill structure approximately 400 feet high. The dam was completed in 1972, and the reservoir was filled by April 1974. The spillway lies along one of the abutments, about one-quarter of a mile from the dam, and is a concrete structure founded on granite.

An analysis was performed to determine an annual frequency of failure for earth, earth-rockfill, and rockfill dams due to events other than overtopping and earthquake ground shaking, which were considered in separate analyses. Also, based on dam design information, structural failure of the spillway during discharge and failure associated with seepage along an outlet works have been eliminated as a possible failure mechanism. The following principal modes of failure were considered:

1. Piping.
2. Seepage.
3. Embankment slides.
4. Structural failure of the foundation or abutments.

These failure mechanisms are referred to collectively as random failures. Only failures resulting in the complete collapse of the structure and the uncontrolled release of the reservoir's contents were considered to have the potential for flooding the Oconee plant.

Previous investigations into the frequency of dam failure indicate that it decreases with later years of construction (Baecher et al., 1980). This is

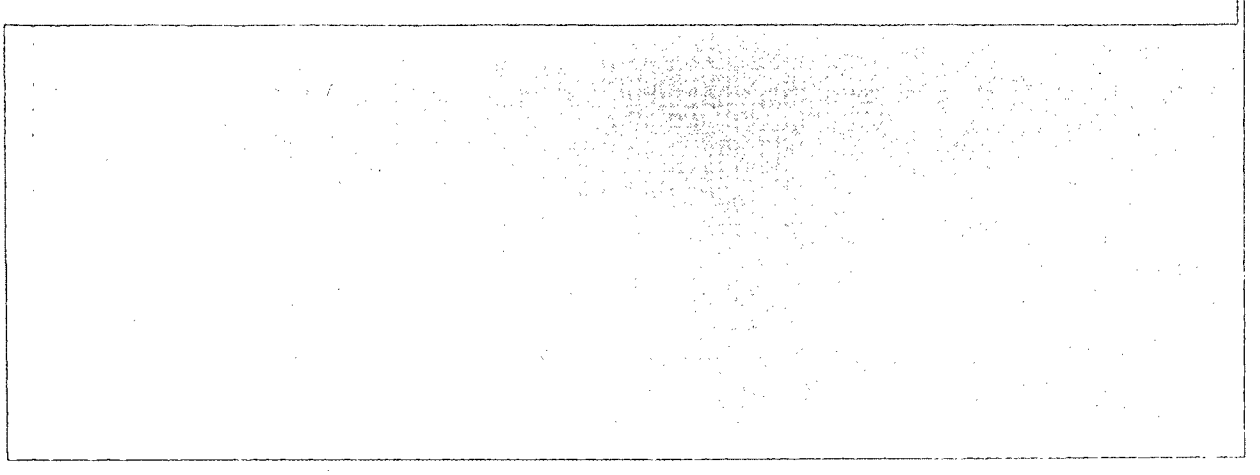

generally attributed to improvements in the methods of design and construction. Therefore, another criterion considered in developing a data base and failure-frequency estimate was the period of construction.

The age of a dam is another factor that has been identified as having an effect on the rate of dam failure. Approximately half the dam failures occur during the first 5 years of operation (Baecher et al., 1980). Therefore, age was also considered in developing a data base.

Size, type of construction, realistic failure modes, period of construction, and age were the major considerations used to define a data base for use in estimating the failure frequency of the Jocassee Dam.

The data-base characteristics that were attributed to the Jocassee Dam are:

Characteristic	Jocassee Dam
Location (country)	United States
Year completed	1972
Age (years in operation)	7
Height (feet)	400
Type	Earth-rockfill

9.4.2.1.1 Data

Various catalogs were used to develop the data groups that were studied. Each group consisted of large earth, earth-rockfill, or rockfill dams (more than 45 feet high, USCOLD, 1975) in the United States that were in operation 6 or more years when they failed. Of the references used in this study (Middlebrooks, 1953; Gruner, 1964; Babb and Mermel, 1968; USCOLD, 1975), not one is a complete catalog, and therefore they were used collectively. At present, these references represent the best readily available information. From the various listings of failures, cross-checks were made when possible.

A data base uniquely suited in every major respect to the Jocassee Dam was unattainable because of a scarcity of the number of the earth-rockfill type.

The data base ultimately developed reflects discussions with Duke Power engineers familiar with the characteristics of the Jocassee Dam. It was decided that the data base should include only the failure modes that could occur at Jocassee. The two major failure types excluded from the data set were failures resulting from piping at a conduit passing through the dam and structural failures of the spillway during the flood discharge. Neither of these failures can occur because the necessary physical conditions do not exist at Jocassee. (Note, however, that dams in the data base do include those that can fail in either or both of these modes. This is proper because the experience from these dams represents realizations of nonfailure for other failure modes, such as embankment piping, foundation failure, and slope failure.)

Because of limitations in the historical record, it is possible only to develop a data set that takes into account a limited number of the specific

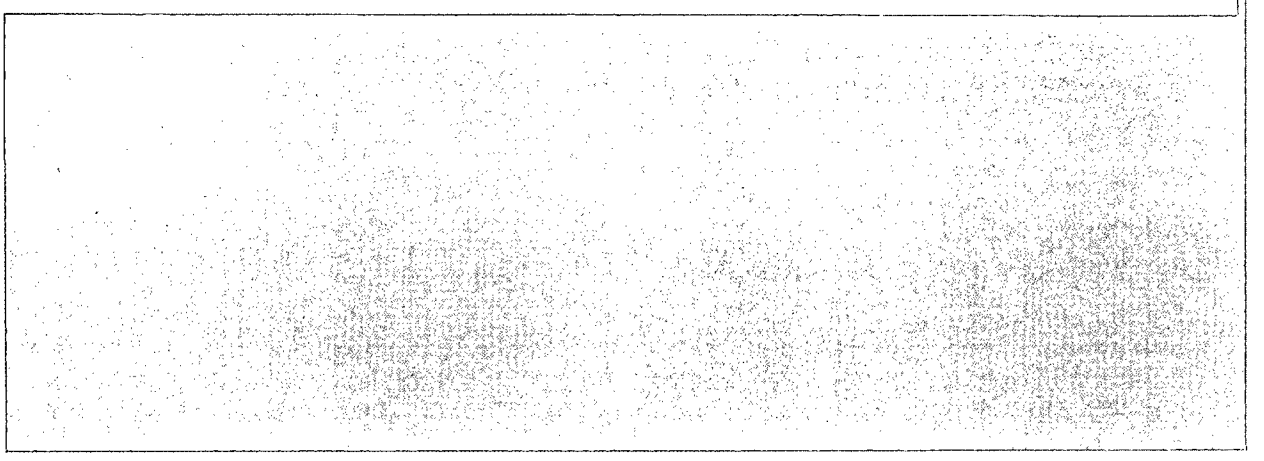

properties of the Jocassee Dam. Since Jocassee is a structure designed and constructed in recent times, it can be assumed that state-of-the-art technology was used in its design. In addition, because of its role as a critical facility of large size and importance, other aspects of the dam, such as seepage monitoring and inspection programs, are important factors that decrease the likelihood that the dam will fail. The following specific characteristics of Jocassee are identified as relevant factors that will affect the frequency of failure:

1. Quality maintenance and inspection programs.
2. Monitoring of the dam (i.e., seepage, settlement, etc.).
3. Presence of personnel at the site.
4. Responsiveness of the owner to potential problems (i.e., implementation of emergency plans).
5. Detailed geologic investigations conducted before site selection.
6. Experience of earth-rockfill dams in Jocassee's class (with respect to random failures).
7. Design techniques.

These factors notwithstanding, the data were examined, and the best available data base for application to Jocassee Dam was extracted (Benjamin and Associates, 1982) and used.

The data base was divided into three overlapping periods of dam construction: 1900 to 1975, 1940 to 1975, and 1960 to 1975. In each category, U.S. dams in operation 6 or more years at the time of failure and 45 feet or more in height were considered. The dams were of three types--earth, earth-rockfill, or rockfill--and only catastrophic failures were included. Table 9-20 lists the failures considered in the analysis.

The number of dam-years of operation was determined from data on the rate of construction provided in the USCOLD (1975) report. Table 9-21 lists chronologically for the three periods of construction the year a failure occurred, the interval between each failure in years, the cumulative number of dam-years to the year of failure, and the number of dam-years between failures.

The data in Table 9-21 show a historically upward trend in the dam-years between catastrophic failures. The reciprocal of these dam-year periods between failures represents the frequency of dam failures. Allowing for statistical variations, this number has been steadily declining since the beginning of this century. This change reflects a steady improvement in the state of the art for the design, construction, and maintenance of dams and dikes (i.e., a "learning curve").

In order to realistically represent the failure rate for a dam of modern design, construction, and operating practice, an analytical method was developed to use the data obtained, including the chronological order of dam failures. The method outlined below is adapted from one first developed by S. Kaplan (personal communication, 1981).

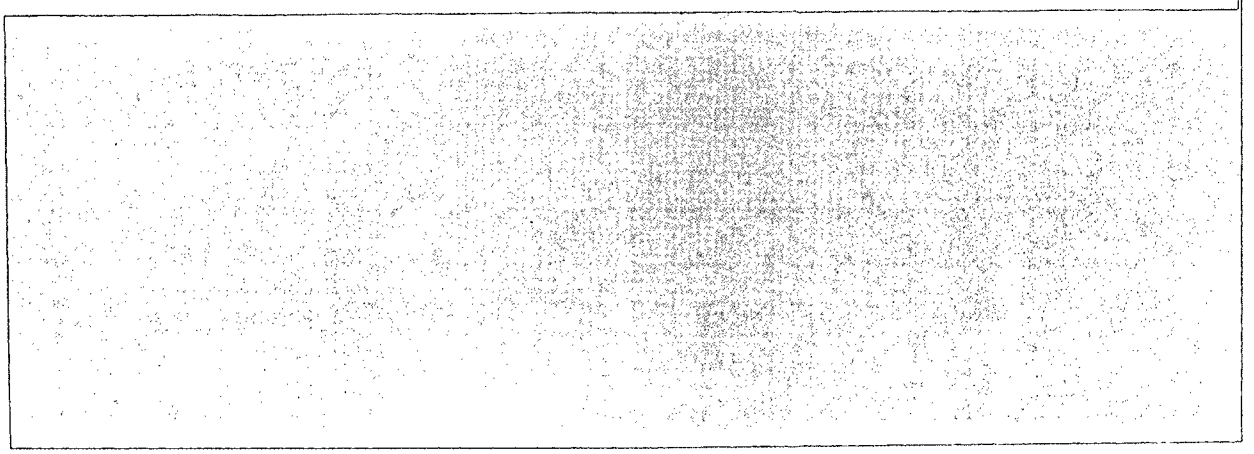

Table 9-20. Dam Failures Used in This Study

Dam	Year completed	Year failed
Goodrich[a]	1900	1956
Lake Toxaway[b]	1902	1916
Sinker Creek[c]	1910	1943
Baldwin Hills[a]	1951	1963
Walter Boudin[d]	1967	1975

[a]Data from Babb and Mermel (1968) and USCOLD (1975).
[b]Data from Babb and Mermel (1968), USCOLD (1975), and Middlebrooks (1953).
[c]Data from Babb and Mermel (1968), Middlebrooks (1953), and USCOLD (1975).
[d]Data from Jansen (1980).

Table 9-21. Chronological Order of Dam Failures

Year of failure	Years between failures	Cumulative dam-years	Dam-years between failures
	Period of Construction: 1900-1975		
1916	16[a]	1,560[a]	1,560[a]
1943	27	15,254	13,694
1956	13	29,236	13,982
1963	7	42,486	13,250
1975	12	82,709	40,223
1981	No failure	107,270	No failure
	Period of Construction: 1940-1975		
1963	23[b]	12,157[b]	12,157[b]
1975	12	43,308	31,151
1981	No failure	67,869	No failure
	Period of Construction: 1960-1975		
1975	15c	18,014[c]	18,014[c]
1981	No failure	42,575	No failure

aFrom 1900.
[b]From 1940.
[c]From 1960.

9.4.2.1.2 Method for Estimating Frequency

The data in Table 9-21 can be regarded as the random realization of a learning process in which the dam-failure frequency evolves with "time" t (measured in dam-years) according to the functional form described by

$$L(t) = at^{-b}$$

In this equation a and b are fitted probabilistically by means of Bayes' theorem. More specifically, a probability distribution on the space of <a,b> doublets, that is, the probability $\{p(a,b|V)\}$ (defined later) was derived. Using this probability distribution, the trend to the "time" (dam-years) accumulated by 1981 was extrapolated to obtain the present-day probability distribution for the frequency of random dam failures.

Method

The functional form chosen to describe the time-dependent (dam-years) failure rate was

$$L(t) = at^{-b} \tag{9.4-14}$$

The probability of no failure between t_{k-1} and t_k, and subsequently a failure at $t_k + dt$ is

$$p(t_{k-1} \rightarrow t_k) = \exp\left\{-\int_{t_{k-1}}^{t_k} L(t)\,dt\right\}\left[L(t_k)\,dt\right]$$

$$= \exp\left\{-\frac{a}{(1-b)}\left[t_k^{(1-b)} - t_{k-1}^{(1-b)}\right]\right\}\left(at_k^{-b}\right) \tag{9.4-15}$$

The probability of experiencing a sequence of K failures is given by the product of the K dam-failure probabilities, where t_o is the time from which the failure and success data have been counted.

$$p(t_o \rightarrow t_k) = \prod_{k=1}^{K} p(t_{k-1} \rightarrow t_k)$$

$$= \prod_{k=1}^{K} \exp\left\{-\frac{a}{(1-b)}\left[t_k^{(1-b)} - t_{k-1}^{(1-b)}\right]\right\}\left(at_k^{-b}\right)$$

$$= a^K \left(\prod_{k=1}^{K} t_k\right)^{-b} \exp\left\{-\frac{a}{(1-b)}\left[t_K^{(1-b)} - t_o^{(1-b)}\right]\right\}(dt)^K \tag{9.4-16}$$

Furthermore, the probability of experiencing a sequence of K failure incidents and subsequently a period of time without failure between the K-th failure time (t_K) and the present time (t_p) is given by

$$p(B|a,b) = p(t_o \rightarrow t_k)\exp\left[-\int_{t_K}^{t_p} L(t)\,dt\right]$$

$$= a^K \left(\prod_{k=1}^{K} t_k\right)^{-b} \exp\left\{-\frac{a}{(1-b)}\left[t_p^{(1-b)} - t_o^{(1-b)}\right]\right\}(dt)^K \tag{9.4-17}$$

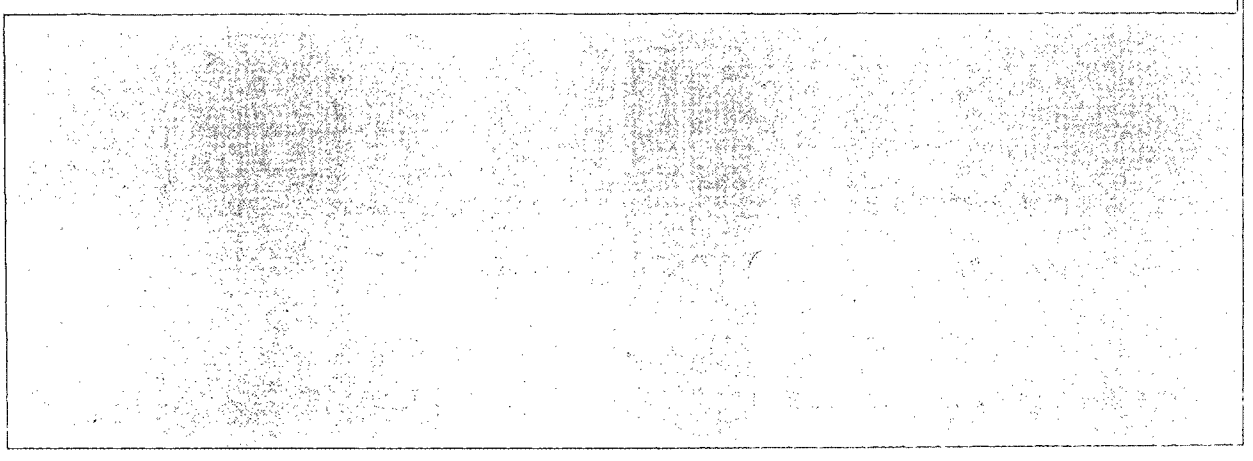

Equation 9.4-17 represents in Bayesian language the likelihood function--that is, the probability of the evidence B (data) given a combination of values for a and b.

Bayes' theorem can be expressed as

$$p(a,b|B) = p(a,b) \frac{p(B|a,b)}{\sum_{\substack{\text{all} \\ a}} \sum_{\substack{\text{all} \\ b}} p(a,b)\ p(B|a,b)} \qquad (9.4\text{-}18)$$

where p(a,b) is the probability of a particular combination of a and b prior to having the evidence B and p(a,b|B) is the probability of a particular combination of a and b posterior to the evidence B (i.e., a measure of the confidence we have in the values of a and b).

Given that prior to evidence B there was no particular preference toward any particular values of a and b, Equation 9.4-18 is then

$$p(a,b|B) = \frac{p(B|a,b)}{\sum_{\substack{\text{all} \\ a}} \sum_{\substack{\text{all} \\ b}} p(B|a,b)} \qquad (9.4\text{-}19)$$

with p(B|a,b) given by Equation 9.4-17.

Numerical Analysis

The numerical procedure involves forming a grid of a_i and b_j values to be used in evaluating p(B|a,b). The process of selecting the grid is somewhat iterative. For the purpose of this analysis, the following grid was arrived at:

$$\{[a_i]\} \equiv \{0.0002, 0.0004, 0.00075, 0.0015, 0.003, 0.006, 0.012, 0.016, 0.02, 0.024, 0.03, 0.04, 0.05, 0.06, 0.075, 0.1\}$$

$$\{[b_j]\} \equiv \{0.1, 0.15, 0.2, 0.25, 0.3, 0.35, 0.4, 0.45, 0.5, 0.55, 0.6, 0.65, 0.7, 0.75, 0.8\}$$

For each combination a_i, b_j from one of these grids, a likelihood $p(B|a_i,b_j)$ can then be calculated from Equation 9.4-17, which we can now express in discrete form:

$$p(B|a_i,b_j) = a_i^K \left(\prod_{k=1}^{K} t_k\right)^{-b_j} \exp\left\{-\frac{a_i}{(1-b_j)}\left[t_p^{(1-b_j)} - t_o^{(1-b_j)}\right]\right\} \qquad (9.4\text{-}20)$$

Finally, a posterior probability for each a_i, b_j can be obtained through a discretely expressed Equation 9.4-19.

$$p(a_i,b_j|B) = \frac{p(B|a_i,b_j)}{\sum_{i=1}^{16} \sum_{j=1}^{15} p(B|a_i,b_j)} \qquad (9.4\text{-}21)$$

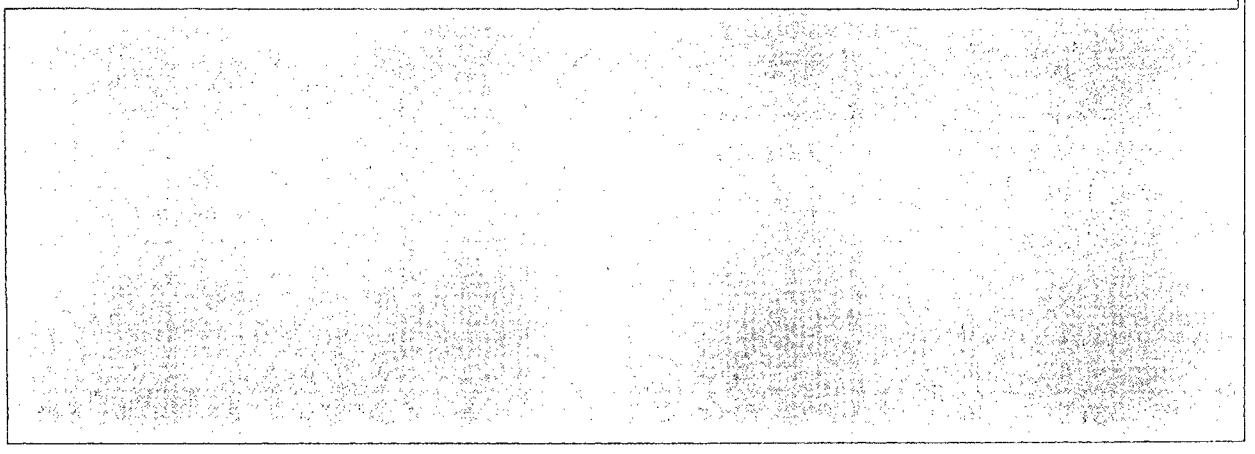

The last step required for completing the analysis is to evaluate Equation 9.4-14 at each one of the grid points (i,j) and time t_p--that is, the dam-years as of 1981 since the last failure in the data base. Again in discrete form Equation 9.4-14 can be written as

$$L_{ij}(t_p) = a_i t_p^{-b_j} \qquad (9.4\text{-}22)$$

Note that for each $L_{ij}(t_p)$ there is a corresponding $p(a_i,b_j|B)$. These corresponding ordered pairs are doublets. The set of

$$\{<p(a_i,b_j|B),L_{ij}(t_p)>\}$$

doublets form a discrete probability distribution that describes the probability of any individual value of dam-failure frequency.

9.4.2.1.3 Results

The numerical analysis outlined in the preceding section was carried out with the objective of estimating the frequency of occurrence and the associated probability for dam failure in 1981. A computer program specifically designed to perform this analysis was written in the Basic language. The results are shown in Table 9-22. The parameters shown are the dam-failure frequency intervals, the discrete probability distribution (DPD) for each frequency interval, and, finally, the cumulative probability from zero to the upper end of each frequency interval.

Table 9-22. Discrete Probability Distribution for Random Dam Failures

Frequency			
From	To	DPD	Cumulative probability
0	8.0-6[a]	0.0519	0.0519
8.0-6[a]	1.0-5	0.0473	0.0993
1.0-5	1.4-5	0.1259	0.2253
1.4-5	1.75-5	0.1199	0.3452
1.75-5	2.2-5	0.1476	0.4928
2.2-5	2.8-5	0.1645	0.6573
2.8-5	3.5-5	0.1188	0.7761
3.5-5	4.4-5	0.1248	0.9010
4.4-5	5.5-5	0.0527	0.9538

[a] $8.0\text{-}6 = 8.0 \times 10^{-6}$.

A plot of the Table 9-22 dam-failure frequency versus cumulative probability yields the 1981 dam-failure frequencies associated with the lower, median, and upper bounds of the probability distribution:

Cumulative probability	1981 annual frequency
0.05	7.9×10^{-6}
0.50	2.3×10^{-5}
0.95	5.5×10^{-5}

The mean annual dam-failure frequency obtained from this distribution is 2.5×10^{-5}.

The analysis indicates that the 1981 mean failure frequency for the class of large U.S. built earthen dams included in the data base described in Section 9.4.2.1.1 is 2.5×10^{-5}. To the extent that this class is representative of the Jocassee Dam, these results can be interpreted as the predicted annual failure frequency of the Jocassee Dam from causes other than earthquakes or overtopping.

In using the data base of Table 9-22 to quantify the dam-failure frequency probability distribution, a fundamental assumption was made: the failure frequency in a particular year for a certain dam (regardless of its age) is identical with the failure frequency of a new dam built in that same year. In other words, the dams that survive up to a given year are just as "good" as the dams built in that year. As a check on the validity of this assumption, a complete learning-curve analysis was done on the subsets of the data base given in Table 9-22. These subsets are represented by the failures of dams built after 1940 and after 1960. The results of these analyses, showing the annual 1981 frequency, are as follows:

Cumulative probability	After-1940 dam	After-1960 dam
0.05	3.2×10^{-6}	1.0×10^{-6}
0.50	1.6×10^{-5}	1.4×10^{-5}
0.95	5.0×10^{-5}	7.7×10^{-5}
Mean	2.0×10^{-5}	2.2×10^{-5}

The median and the mean values of the 1981 dam-failure frequencies obtained by using different subsets of the failure data base compare closely. As expected, the bounds of the distribution are tighter as more data are included. These comparisons indicate that the above-mentioned assumption is reasonable.

9.4.2.2 Contribution to Core-Melt Frequency

In order to evaluate the contribution of random failure of Jocassee Dam to the frequency of core melt at Oconee Unit 3, three factors must be quanti-

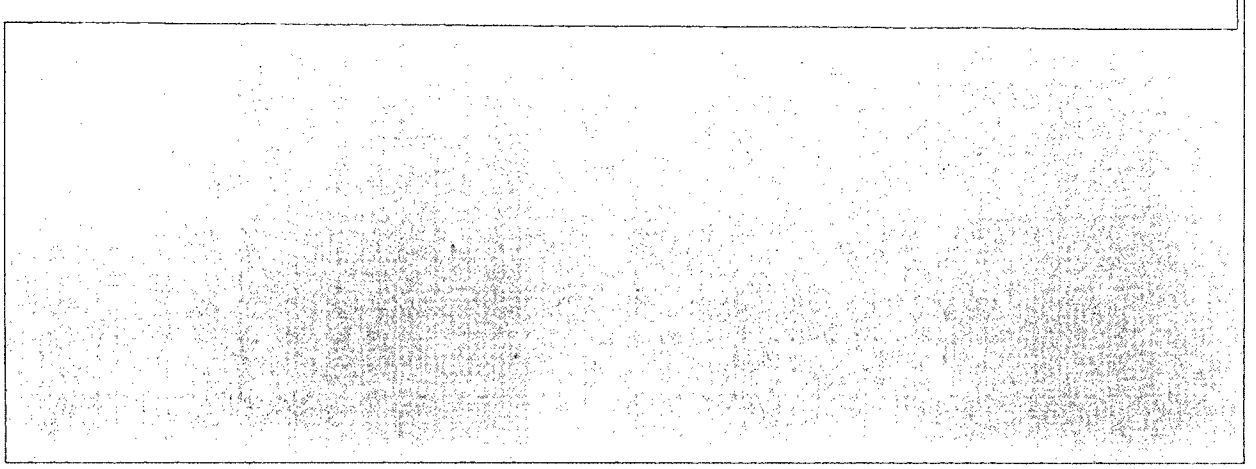

fied. The first factor, the frequency of random dam failures, was estimated in the preceding section. The remaining two factors are the following:

1. The conditional probability of flooding of the Oconee site given a failure of the Jocassee Dam.

2. The conditional probability of core melt given flooding at the Oconee site.

The conditional probability of flooding at the Oconee site given a failure of the Jocassee Dam is a complex function of several variables. The level of the Jocassee Lake at the time of failure determines the amount of impounded water that will be released into Lake Keowee; the level of Lake Keowee determines how much flow can be received from Lake Jocassee before Keowee Dam and the Oconee intake dike are overtopped. The time available for warning of an impending dam failure will determine the likelihood that effective action can be taken to lower the levels of the Jocassee and Keowee Lakes and whether an action like notching the east side of the Keowee Dam, allowing the flood to bypass the Oconee site, could be conceived and implemented. The conditional probability of flooding given a dam failure also depends on the mode of failure, the rate of erosion (time to failure), the vertical depth to which the failure penetrates (fraction of the impounded water released), and whether either Keowee Dam or the east intake dike fails rapidly when overtopped (allowing the flood to bypass the Oconee site).

The data base includes only catastrophic failures by modes believed applicable to Jocassee. Most of the catastrophic failures reported in the literature for earth or earth-rockfill dams were total (i.e., the entire reservoir emptied), and most times to failure were in the range of 1 to 2 hours. However, the failures in the data base (Table 9-20) occurred only in earthen dams; thus, there is some question as to how applicable their rates of erosion and depths of failure are to the Jocassee Dam, an earth-rockfill structure.

The Hell Hole Dam, an earth-rockfill structure, failed during construction in 1964 when extreme precipitation caused overtopping. Since construction had not been completed and since the dam was overtopped, it did not satisfy the data-base characteristics and was not included in the failure set. However, its material of construction and size were very similar to those of Jocassee, and its failure behavior can therefore be used as one point of reference in judgments about the possible failure behavior of Jocassee. The overtopping of this partly constructed dam lasted for more than 40 hours before a catastrophic failure occurred. This suggests that a long warning time may be available, at least in some cases, before the failure of an earth-rockfill dam. Once the dam was breached, however, the breach propagated the full depth of the dam, down to the foundation, in about 2 hours. Thus, though more warning time may have been available, once failure began, the time and depth to complete breach were quite similar to those observed for earthen dams.

In addition to the uncertainty in the important parameters described above, a spectrum of calculated flood levels is not available. Thus it is not possible to determine where the sensitive range for the key parameters lies. Given this lack of information, a bounding value of 1 was used for the conditional probability of flooding of the Oconee site given a catastrophic failure of the Jocassee Dam.

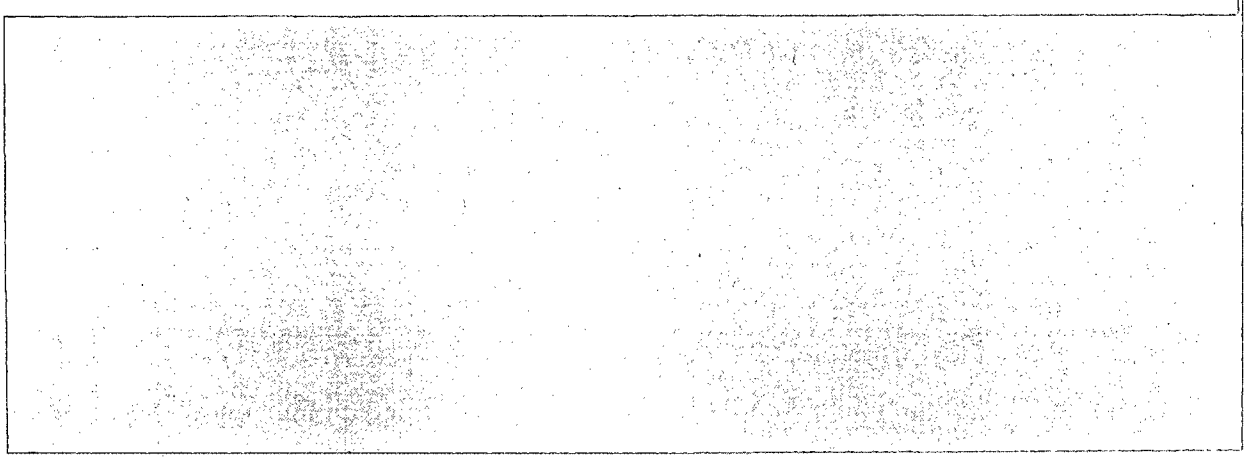

The conditional probability of core melt given flooding at the Oconee site is also a complex function depending on the warning time, the action taken by the plant staff (e.g., hot shutdown vs. cold shutdown; whether the standby shutdown facility is manned), the depth of flooding, the survival time for various plant equipment (e.g., steam-driven emergency feedwater pump, standby shutdown facility), and other factors. A scoping of this problem indicates that all means of core cooling are likely to be lost for more than 24 hours, and a conditional probability of 1 was assigned to core melt given flooding.

Combining the three factors yields a bounding estimate of 2.5×10^{-5} for the mean annual frequency of core melt due to a random failure of the Jocassee Dam. It is possible that a more detailed analysis could provide estimated conditional probabilities of site flooding and core melt less than unity. However, core melt due to flooding in the turbine building from CCW failures clearly dominates the contribution from dam failure, and further analysis was judged to be not warranted.

A scoping analysis was performed to investigate whether or not an interfacing-system LOCA could be caused by a loss of decay-heat removal due to the flood, and subsequent RCS heatup and pressurization. Assuming core cooling is lost at about 8 hours after a reactor trip with the plant in a cooled-down condition and the PORV reset to lift at approximately 500 psig, decay heat could be matched with liquid relief at system pressure on the order of 100 psia. Several hours would be required to heat up the primary and secondary systems. In steady state at about 12 hours after a trip and after significant RCS inventory has been lost through liquid relief, saturated steam relief out of the RCS via the PORV at about 500 psia could match the decay heat, and the RCS would stabilize at a pressure below that estimated to cause a rupture in the 388-psig design RHR suction piping. Therefore it was concluded that a core melt caused by the flooding of the plant and a prolonged loss of core cooling would not directly breach the containment. Since this sequence would be a late core melt (on the order of 12 hours) with the RCS at moderate pressure (about 500 psig), it was assigned to core-melt bin II. Flood effects would cause a failure of the reactor-building sprays and cooling units (i.e., containment-safeguard state C). Thus these sequences were assigned to plant-damage bin IIC.